US007467002B2

(12) **United States Patent**
Weber et al.

(10) **Patent No.: US 7,467,002 B2**
(45) **Date of Patent: Dec. 16, 2008**

(54) **SINE SATURATION TRANSFORM**

(75) Inventors: **Walter M. Weber**, Dana Point, CA (US); **Ammar Al-All**, Tustin, CA (US); **Lorenzo Cazzoll**, Barcelona (ES)

(73) Assignee: **Masimo Corporation**, Irvine, CA (US)

(*) Notice: Subject to any disclaimer, the term of this patent is extended or adjusted under 35 U.S.C. 154(b) by 0 days.

(21) Appl. No.: **11/894,648**

(22) Filed: **Aug. 20, 2007**

(65) **Prior Publication Data**

US 2008/0045810 A1 Feb. 21, 2008

Related U.S. Application Data

(63) Continuation of application No. 11/417,914, filed on May 3, 2006, which is a continuation of application No. 11/048,232, filed on Feb. 1, 2005, which is a continuation of application No. 10/184,032, filed on Jun. 26, 2002, now Pat. No. 6,850,787.

(60) Provisional application No. 60/302,438, filed on Jun. 29, 2001.

(51) **Int. Cl.**
A61B 5/145 (2006.01)

(52) **U.S. Cl.** **600/324**; 600/323; 702/190

(58) **Field of Classification Search** 600/322, 600/323, 324; 702/189, 190
See application file for complete search history.

(56) **References Cited**

U.S. PATENT DOCUMENTS

4,960,128	A	10/1990	Gordon et al.
4,964,408	A	10/1990	Hink et al.
5,041,187	A	8/1991	Hink et al.
5,069,213	A	12/1991	Polczynski
5,163,438	A	11/1992	Gordon et al.
5,337,744	A	8/1994	Branigan
5,341,805	A	8/1994	Stavridi et al.
D353,195	S	12/1994	Savage et al.
D353,196	S	12/1994	Savage et al.
5,377,676	A	1/1995	Vari et al.
D359,546	S	6/1995	Savage et al.
5,431,170	A	7/1995	Mathews

(Continued)

FOREIGN PATENT DOCUMENTS

WO	WO 98/42250	10/1998

(Continued)

OTHER PUBLICATIONS

Office Action of Japanese Patent Application No. 2003-508244 dated Mar. 26, 2008 and English Translation of same in 35 pages.

(Continued)

Primary Examiner—Eric F Winakur
Assistant Examiner—Etsub D Berhanu
(74) *Attorney, Agent, or Firm*—Knobbe, Martens, Olson & Bear LLP

(57) **ABSTRACT**

A transform for determining a physiological measurement is disclosed. The transform determines a basis function index from a physiological signal obtained through a physiological sensor. A basis function waveform is generated based on basis function index. The basis function waveform is then used to determine an optimized basis function waveform. The optimized basis function waveform is used to calculate a physiological measurement.

14 Claims, 14 Drawing Sheets

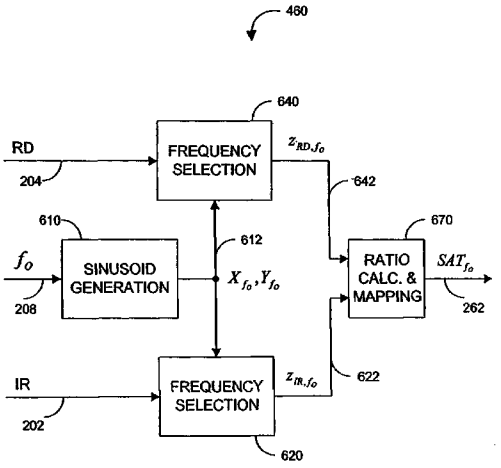

U.S. PATENT DOCUMENTS

D361,840	S		8/1995	Savage et al.
D362,063	S		9/1995	Savage et al.
5,452,717	A		9/1995	Branigan et al.
D363,120	S		10/1995	Savage et al.
5,456,252	A		10/1995	Vari et al.
5,482,036	A		1/1996	Diab et al.
5,490,505	A		2/1996	Diab et al.
5,494,043	A		2/1996	O'Sullivan et al.
5,533,511	A		7/1996	Kaspari et al.
5,561,275	A		10/1996	Savage et al.
5,562,002	A		10/1996	Lalin
5,590,649	A		1/1997	Caro et al.
5,602,924	A		2/1997	Durand et al.
5,632,272	A		5/1997	Diab et al.
5,638,816	A		6/1997	Kiani-Azarbayjany et al.
5,638,818	A		6/1997	Diab et al.
5,645,440	A		7/1997	Tobler et al.
5,685,299	A		11/1997	Diab et al.
D393,830	S		4/1998	Tobler et al.
5,743,262	A		4/1998	Lepper, Jr. et al.
5,758,644	A		6/1998	Diab et al.
5,760,910	A		6/1998	Lepper, Jr. et al.
5,769,785	A		6/1998	Diab et al.
5,782,757	A		7/1998	Diab et al.
5,785,659	A		7/1998	Caro et al.
5,791,347	A		8/1998	Flaherty et al.
5,810,734	A		9/1998	Caro et al.
5,823,950	A		10/1998	Diab et al.
5,830,131	A		11/1998	Caro et al.
5,833,618	A		11/1998	Caro et al.
5,853,364	A	*	12/1998	Baker et al. 600/300
5,860,919	A		1/1999	Kiani-Azarbayjany et al.
5,890,929	A		4/1999	Mills et al.
5,904,654	A		5/1999	Wohltmann et al.
5,919,134	A		7/1999	Diab
5,934,925	A		8/1999	Tobler et al.
5,940,182	A		8/1999	Lepper, Jr. et al.
5,995,855	A		11/1999	Kiani et al.
5,997,343	A		12/1999	Mills et al.
6,002,952	A		12/1999	Diab et al.
6,011,986	A		1/2000	Diab et al.
6,027,452	A		2/2000	Flaherty et al.
6,036,642	A		3/2000	Diab et al.
6,045,509	A		4/2000	Caro et al.
6,067,462	A		5/2000	Diab et al.
6,081,735	A		6/2000	Diab et al.
6,088,607	A		7/2000	Diab et al.
6,110,522	A		8/2000	Lepper, Jr. et al.
6,124,597	A		9/2000	Shehada
6,144,868	A		11/2000	Parker
6,151,516	A		11/2000	Kiani-Azarbayjany et al.
6,152,754	A		11/2000	Gerhardt et al.
6,157,850	A		12/2000	Diab et al.
6,165,005	A		12/2000	Mills et al.
6,184,521	B1		2/2001	Coffin, IV et al.
6,206,830	B1		3/2001	Diab et al.
6,229,856	B1		5/2001	Diab et al.
6,232,609	B1		5/2001	Snyder et al.
6,236,872	B1		5/2001	Diab et al.
6,241,683	B1		6/2001	Macklem et al.
6,256,523	B1		7/2001	Diab et al.
6,263,222	B1		7/2001	Diab et al.
6,278,522	B1		8/2001	Lepper, Jr. et al.
6,280,213	B1		8/2001	Tobler et al.
6,285,896	B1		9/2001	Tobler et al.
6,321,100	B1		11/2001	Parker
6,334,065	B1		12/2001	Al-Ali et al.
6,343,224	B1		1/2002	Parker
6,349,228	B1		2/2002	Kiani et al.
6,360,114	B1		3/2002	Diab et al.
6,368,283	B1		4/2002	Xu et al.
6,371,921	B1		4/2002	Caro et al.
6,377,829	B1		4/2002	Al-Ali
6,388,240	B2		5/2002	Schulz et al.
6,397,091	B2		5/2002	Diab et al.
6,430,525	B1		8/2002	Weber et al.
6,463,311	B1		10/2002	Diab
6,470,199	B1		10/2002	Kopotic et al.
6,501,975	B2		12/2002	Diab et al.
6,505,059	B1		1/2003	Kollias et al.
6,515,273	B2		2/2003	Al-Ali
6,519,486	B1	*	2/2003	Edgar et al. 600/336
6,519,487	B1		2/2003	Parker
6,525,386	B1		2/2003	Mills et al.
6,526,300	B1		2/2003	Kiani et al.
6,541,756	B2		4/2003	Schulz et al.
6,542,764	B1		4/2003	Al-Ali et al.
6,580,086	B1		6/2003	Schulz et al.
6,584,336	B1		6/2003	Ali et al.
6,595,316	B2		7/2003	Cybulski et al.
6,597,932	B2		7/2003	Tian et al.
6,597,933	B2		7/2003	Kiani et al.
6,606,511	B1		8/2003	Ali et al.
6,632,181	B2		10/2003	Flaherty et al.
6,639,668	B1		10/2003	Trepagnier
6,640,116	B2		10/2003	Diab
6,643,530	B2		11/2003	Diab et al.
6,650,917	B2		11/2003	Diab et al.
6,654,624	B2		11/2003	Diab et al.
6,658,276	B2		12/2003	Kianl et al.
6,661,161	B1		12/2003	Lanzo et al.
6,671,531	B2		12/2003	Al-Ali et al.
6,678,543	B2		1/2004	Diab et al.
6,684,090	B2		1/2004	Ali et al.
6,684,091	B2		1/2004	Parker
6,697,656	B1		2/2004	Al-Ali
6,697,657	B1		2/2004	Shehada et al.
6,697,658	B2		2/2004	Al-Ali
RE38,476	E		3/2004	Diab et al.
6,699,194	B1		3/2004	Diab et al.
6,714,804	B2		3/2004	Al-Ali et al.
RE38,492	E		4/2004	Diab et al.
6,721,582	B2		4/2004	Trepagnier et al.
6,721,585	B1		4/2004	Parker
6,725,075	B2		4/2004	Al-Ali
6,728,560	B2		4/2004	Kollias et al.
6,735,459	B2		5/2004	Parker
6,745,060	B2		6/2004	Diab et al.
6,760,607	B2		7/2004	Al-All
6,770,028	B1		8/2004	Ali et al.
6,771,994	B2		8/2004	Kiani et al.
6,792,300	B1		9/2004	Diab et al.
6,813,511	B2		11/2004	Diab et al.
6,816,741	B2		11/2004	Diab
6,822,564	B2		11/2004	Al-Ali
6,826,419	B2		11/2004	Diab et al.
6,830,711	B2		12/2004	Mills et al.
6,850,787	B2		2/2005	Weber et al.
6,850,788	B2		2/2005	Al-Ali
6,852,083	B2		2/2005	Caro et al.
6,861,639	B2		3/2005	Al-Ali
6,898,452	B2		5/2005	Al-Ali et al.
6,920,345	B2		7/2005	Al-Ali et al.
6,931,268	B1		8/2005	Kiani-Azarbayjany et al.
6,934,570	B2		8/2005	Kiani et al.
6,939,305	B2		9/2005	Flaherty et al.
6,943,348	B1		9/2005	Coffin IV
6,950,687	B2		9/2005	Al-Ali
6,961,598	B2		11/2005	Diab
6,970,792	B1		11/2005	Diab
6,979,812	B2		12/2005	Al-Ali
6,985,764	B2		1/2006	Mason et al.
6,993,371	B2		1/2006	Kiani et al.
6,996,427	B2		2/2006	Ali et al.

6,999,904	B2	2/2006	Weber et al.
7,003,338	B2	2/2006	Weber et al.
7,003,339	B2	2/2006	Diab et al.
7,015,451	B2	3/2006	Dalke et al.
7,024,233	B2	4/2006	Ali et al.
7,027,849	B2	4/2006	Al-Ali
7,030,749	B2	4/2006	Al-Ali
7,039,449	B2	5/2006	Al-Ali
7,041,060	B2	5/2006	Flaherty et al.
7,044,918	B2	5/2006	Diab
7,067,893	B2	6/2006	Mills et al.
7,096,052	B2	8/2006	Mason et al.
7,096,054	B2	8/2006	Abdul-Hafiz et al.
7,132,641	B2	11/2006	Schulz et al.
7,142,901	B2	11/2006	Kiani et al.
7,149,561	B2	12/2006	Diab
7,186,966	B2	3/2007	Al-Ali
7,190,261	B2	3/2007	Al-Ali
7,215,984	B2	5/2007	Diab
7,215,986	B2	5/2007	Diab
7,221,971	B2	5/2007	Diab
7,225,006	B2	5/2007	Al-Ali et al.
7,225,007	B2	5/2007	Al-Ali
RE39,672	E	6/2007	Shehada et al.
7,239,905	B2	7/2007	Kiani-Azarbayjany et al.
7,245,953	B1	7/2007	Parker
7,254,431	B2	8/2007	Al-Ali
7,254,433	B2	8/2007	Diab et al.
7,254,434	B2	8/2007	Schulz et al.
7,272,425	B2	9/2007	Al-Ali
7,274,955	B2	9/2007	Kiani et al.
D554,263	S	10/2007	Al-Ali
7,280,858	B2	10/2007	Al-Ali et al.
7,289,835	B2	10/2007	Mansfield et al.
7,292,883	B2	11/2007	De Felice et al.
7,295,866	B2	11/2007	Al-Ali
7,328,053	B1	2/2008	Diab et al.
7,332,784	B2	2/2008	Mills et al.
7,340,287	B2	3/2008	Mason et al.
7,341,559	B2	3/2008	Schulz et al.
7,343,186	B2	3/2008	Lamego et al.
D566,282	S	4/2008	Al-Ali et al.
7,355,512	B1	4/2008	Al-Ali
7,371,981	B2	5/2008	Abdul-Hafiz
7,373,193	B2	5/2008	Al-Ali et al.
7,373,194	B2	5/2008	Weber et al.
7,376,453	B1	5/2008	Diab et al.
7,377,794	B2	5/2008	Al-Ali et al.
7,377,899	B2	5/2008	Weber et al.
7,383,070	B2	6/2008	Diab et al.

FOREIGN PATENT DOCUMENTS

WO	WO 02/047582 A3	6/2002

OTHER PUBLICATIONS

PCT International Search Report, App. No. PCT/US 02/20674, App. Dates: Jun. 28, 2002, 5 pages.

Office Action of Japanese Patent Application No. 2003-508244 Dispatched on Mar. 26, 2008 and English Translation of same in 35 pages.

* cited by examiner

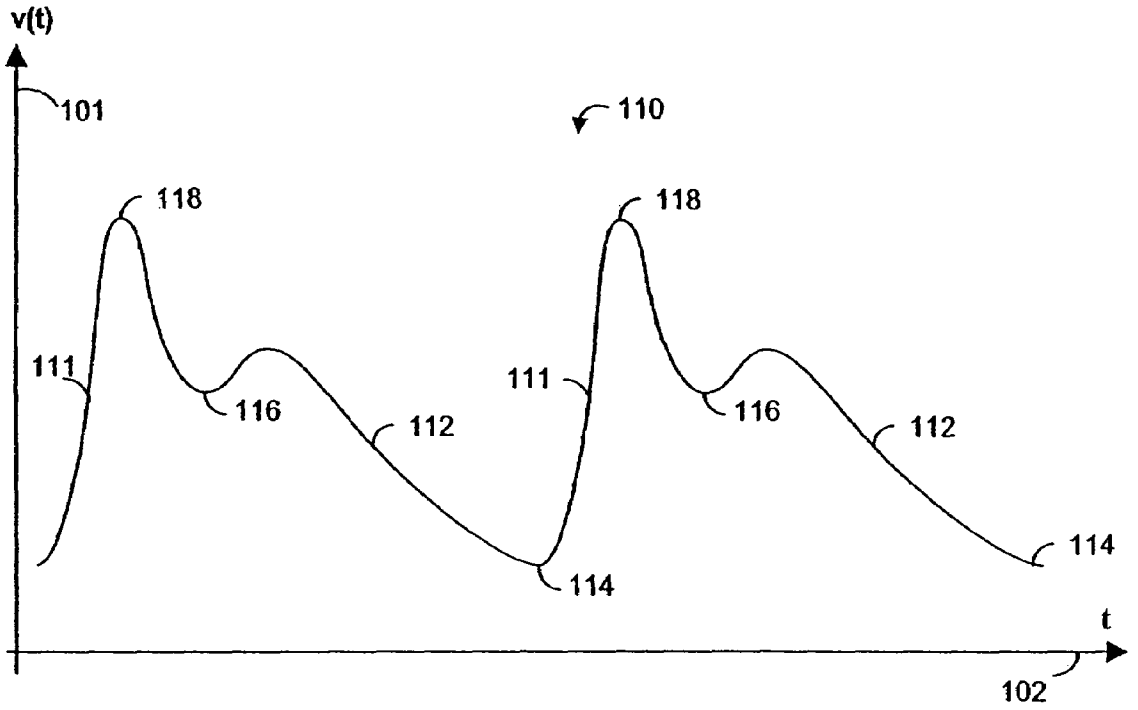

FIG. 1A

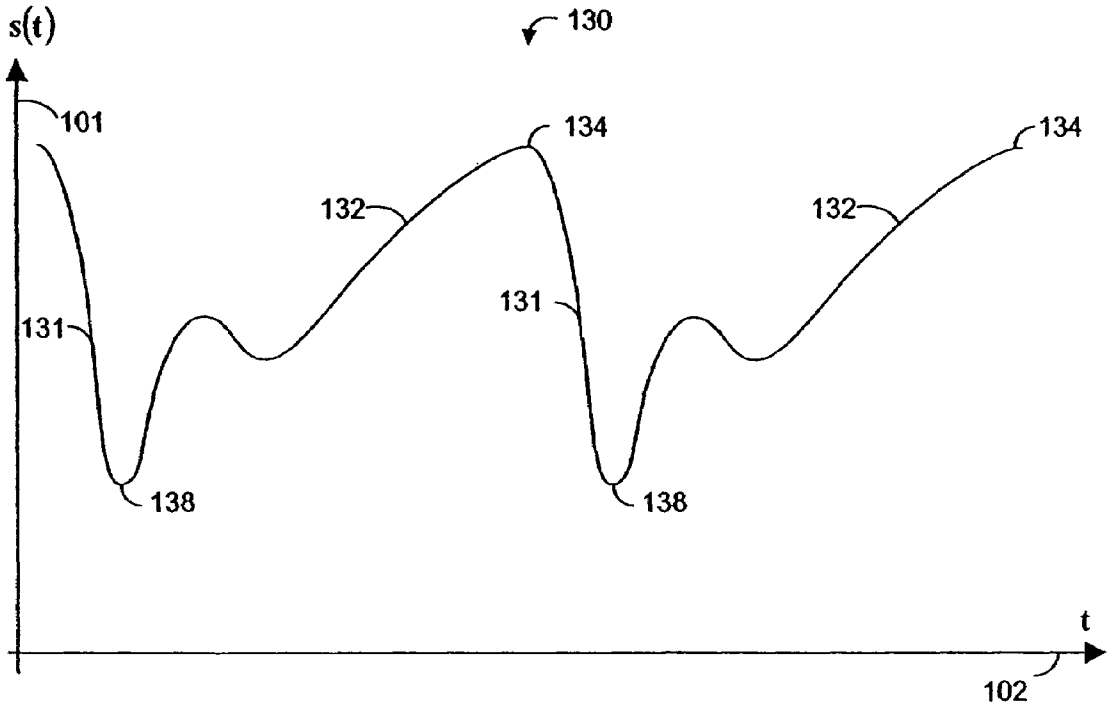

FIG. 1B

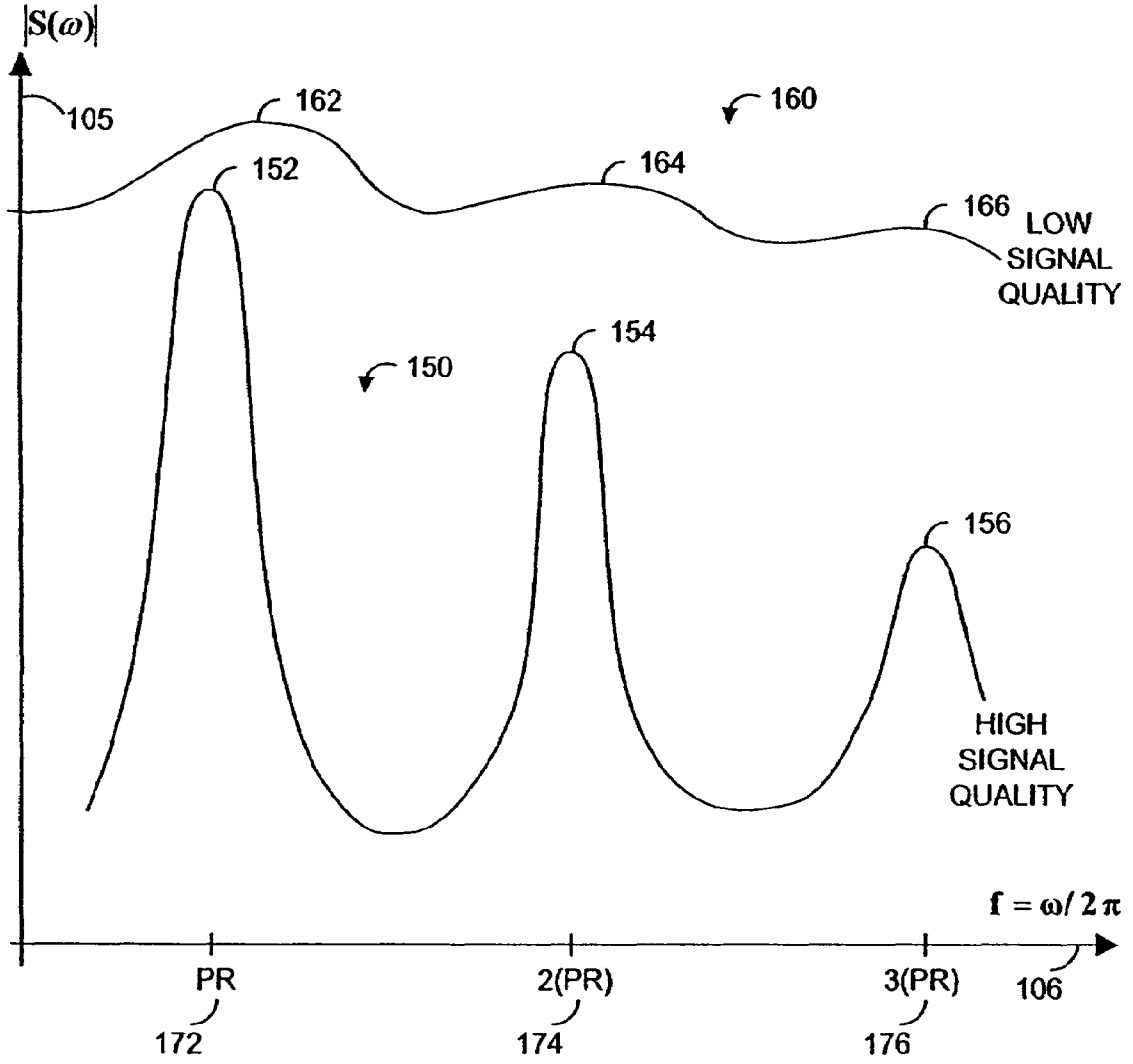
|S(ω)|
105
162
160
152
164
166
LOW
SIGNAL
QUALITY
150
154
156
HIGH
SIGNAL
QUALITY
f = ω/2π
PR
2(PR)
3(PR)
106
172
174
176

FIG. 1C

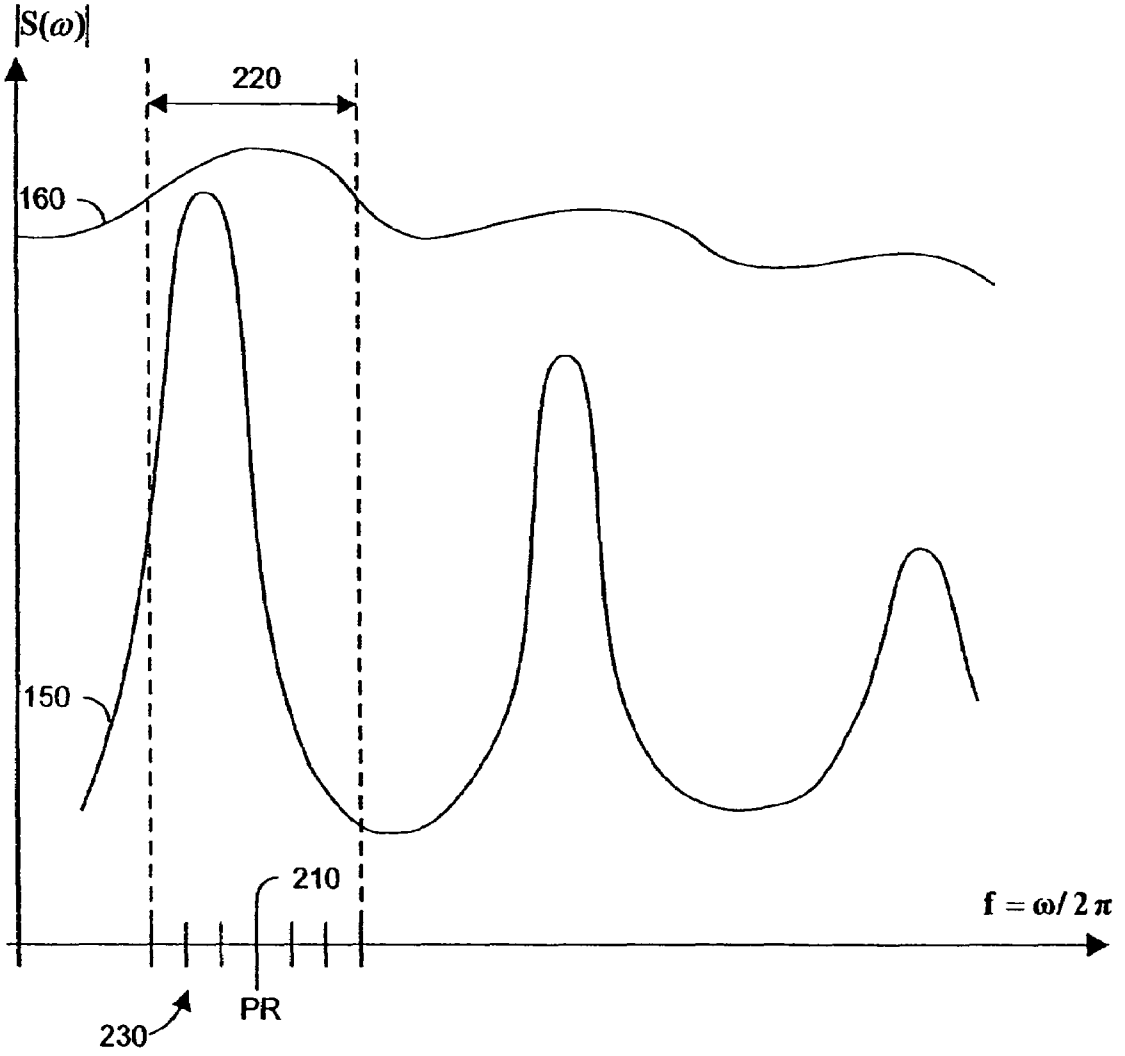

FIG. 2

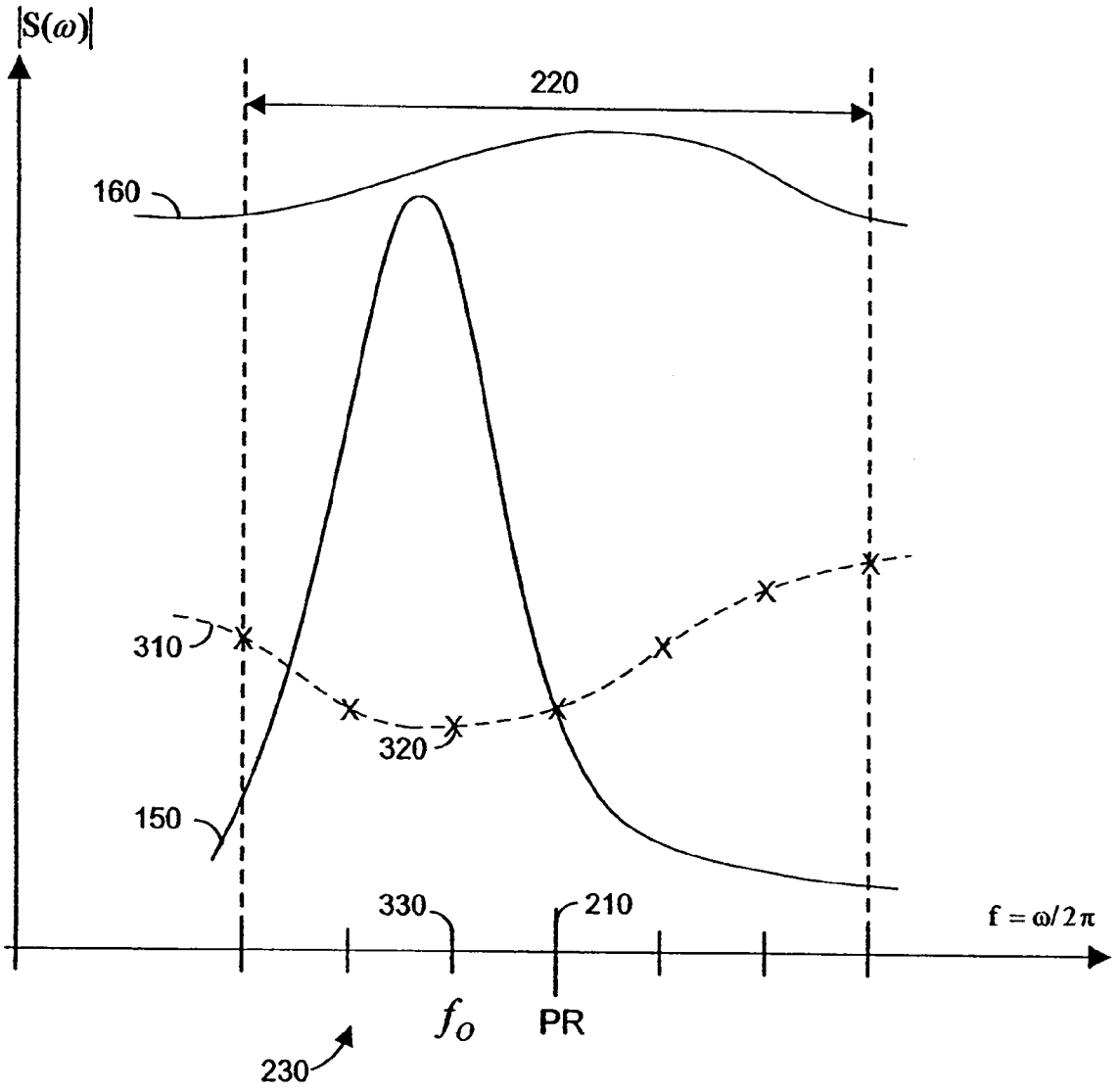

FIG. 3

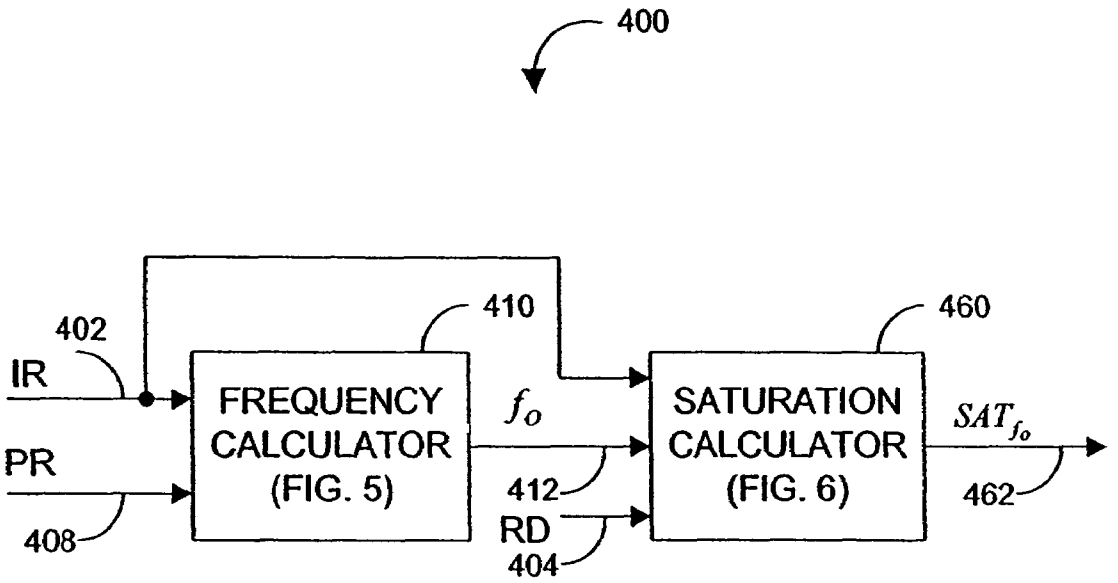
400
402
IR
PR
408
410
FREQUENCY CALCULATOR (FIG. 5)
f_o
412
RD
404
460
SATURATION CALCULATOR (FIG. 6)
SAT_{f_o}
462

FIG. 4

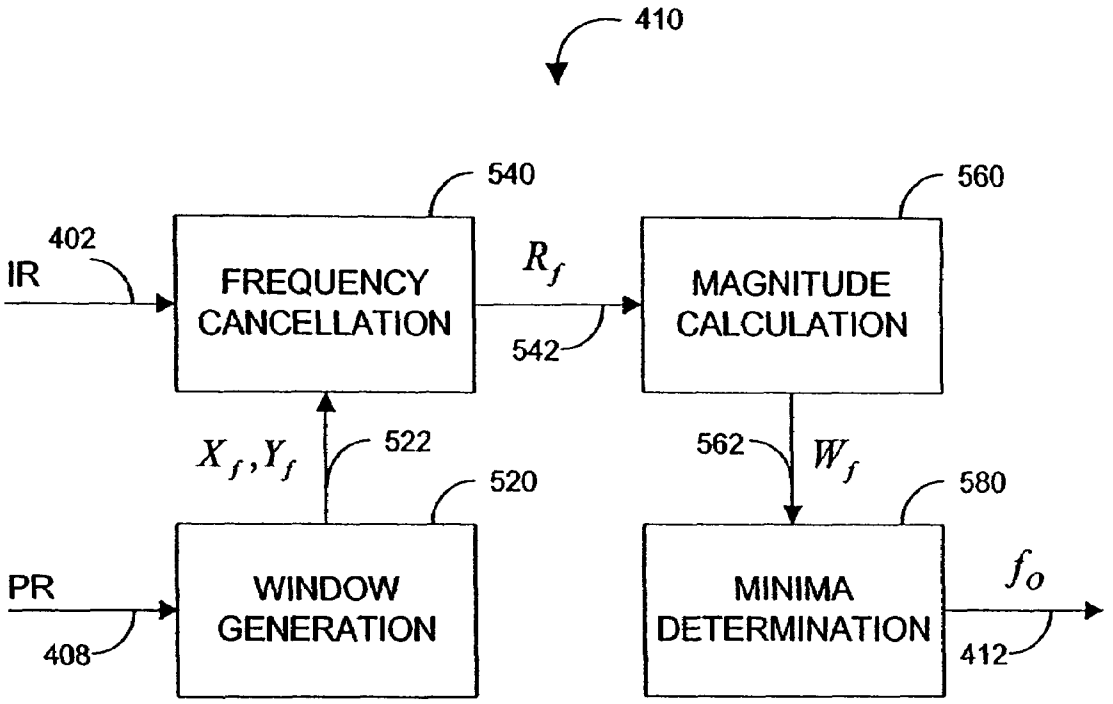
410
540
560
402
IR
FREQUENCY CANCELLATION
R_f
MAGNITUDE CALCULATION
542
X_f, Y_f
522
562
W_f
520
580
PR
WINDOW GENERATION
MINIMA DETERMINATION
f_o
408
412

FIG. 5

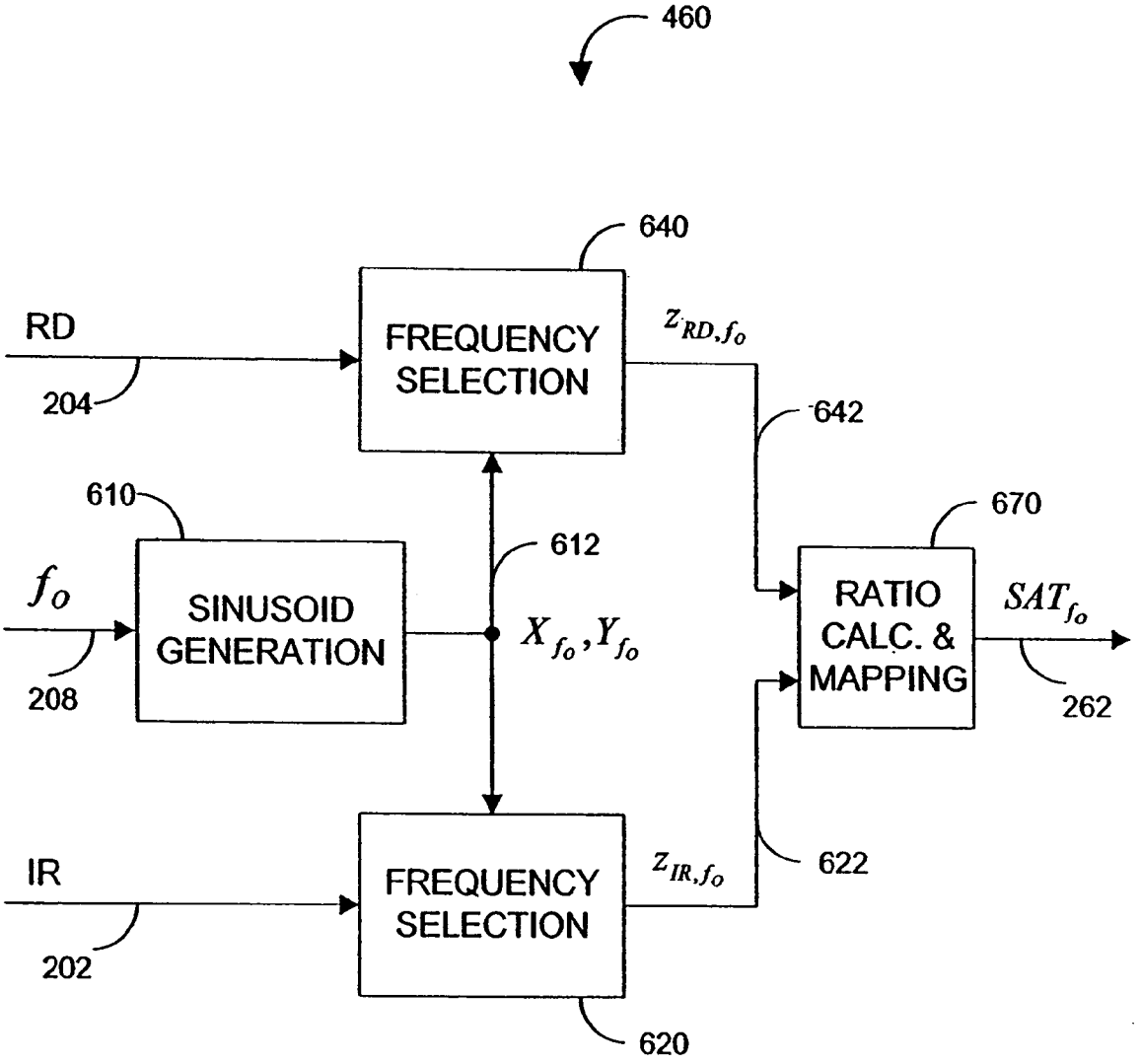
460
640
RD
204
FREQUENCY SELECTION
Z_{RD,f_o}
642
610
670
612
f_o
208
SINUSOID GENERATION
X_{f_o}, Y_{f_o}
RATIO CALC. & MAPPING
SAT_{f_o}
262
IR
202
FREQUENCY SELECTION
Z_{IR,f_o}
622
620

FIG. 6

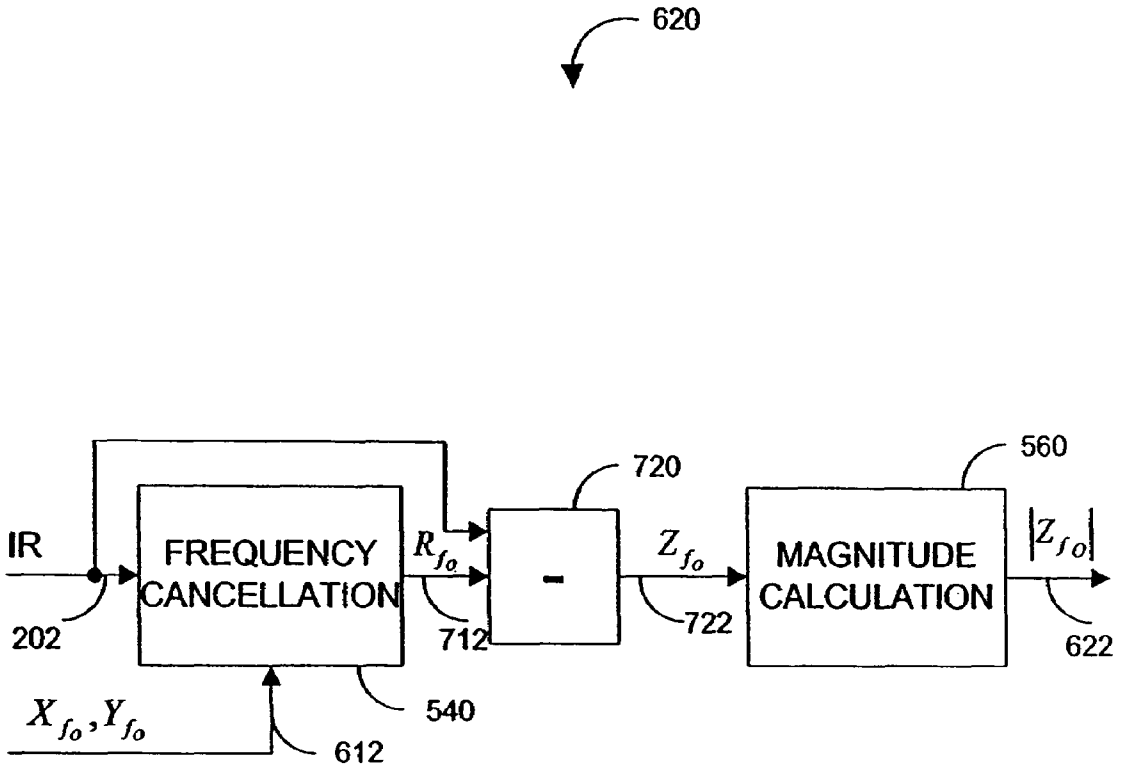
620
IR
202
FREQUENCY CANCELLATION
R_{fo}
712
720
-
Z_{fo}
722
560
MAGNITUDE CALCULATION
$|Z_{fo}|$
622
540
X_{fo}, Y_{fo}
612

FIG. 7

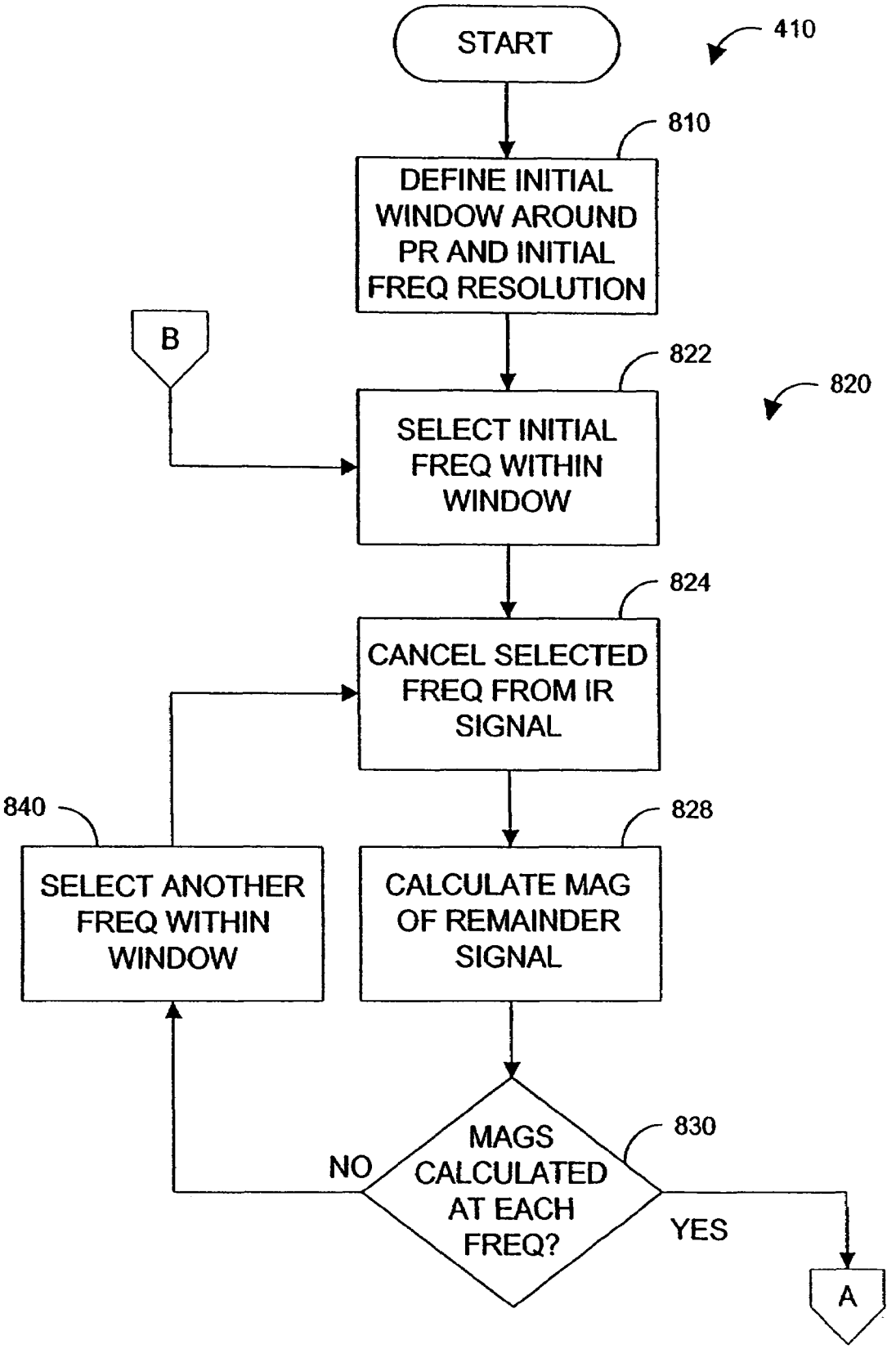
START
410
810
DEFINE INITIAL WINDOW AROUND PR AND INITIAL FREQ RESOLUTION
B
822
820
SELECT INITIAL FREQ WITHIN WINDOW
824
CANCEL SELECTED FREQ FROM IR SIGNAL
840
828
SELECT ANOTHER FREQ WITHIN WINDOW
CALCULATE MAG OF REMAINDER SIGNAL
830
MAGS CALCULATED AT EACH FREQ?
NO
YES
A

FIG. 8A

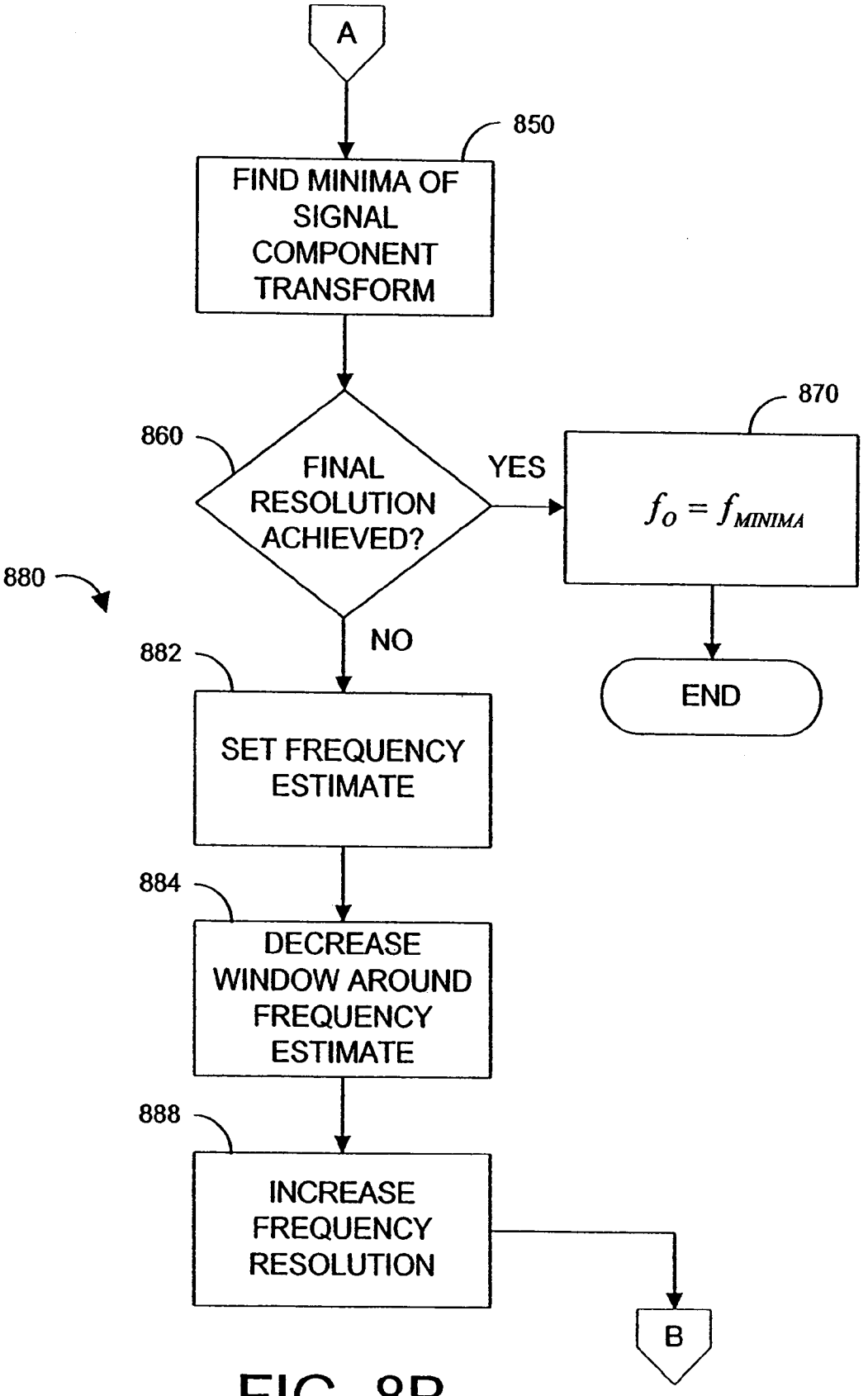
A
850
FIND MINIMA OF SIGNAL COMPONENT TRANSFORM
860
FINAL RESOLUTION ACHIEVED?
YES
870
$f_o = f_{MINIMA}$
880
NO
END
882
SET FREQUENCY ESTIMATE
884
DECREASE WINDOW AROUND FREQUENCY ESTIMATE
888
INCREASE FREQUENCY RESOLUTION
B

FIG. 8B

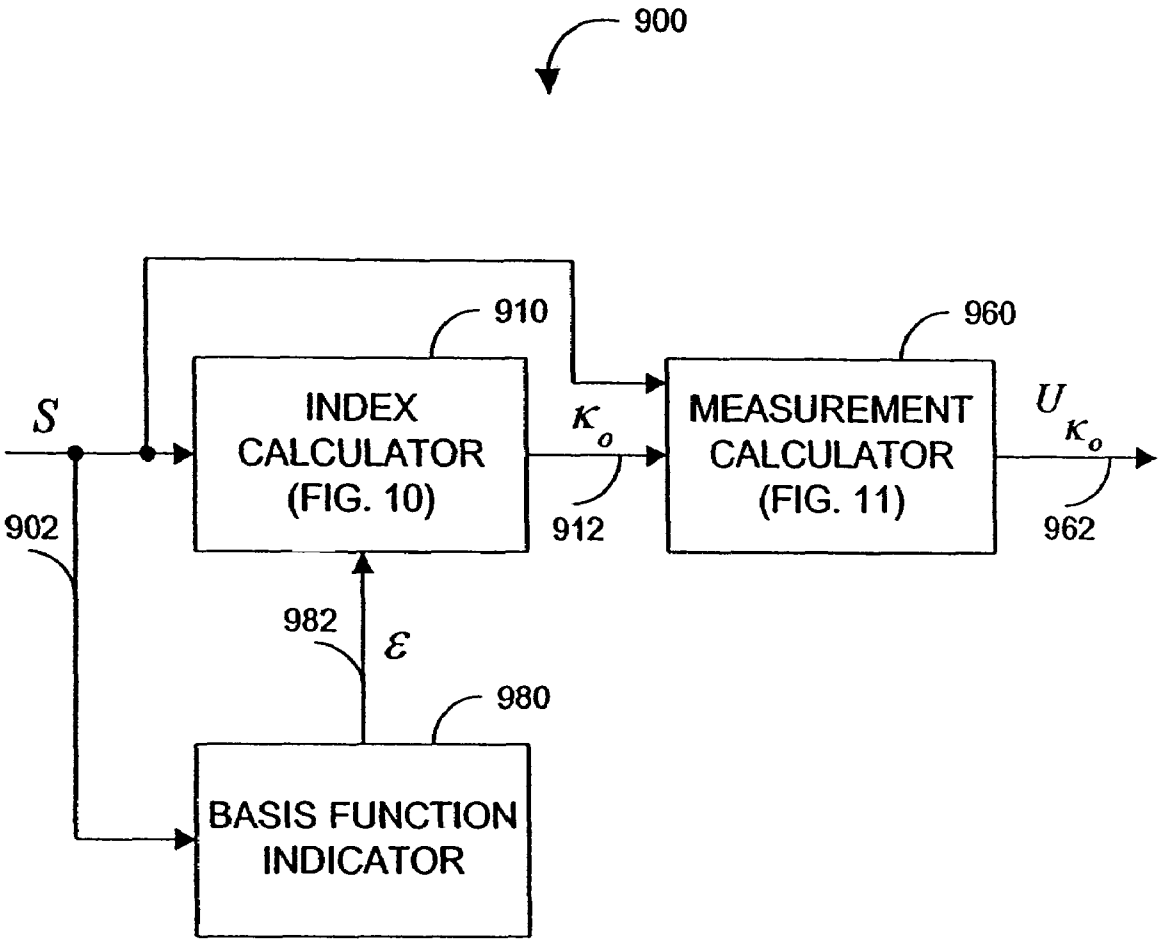
900
910
960
S
INDEX CALCULATOR (FIG. 10)
κ_o
MEASUREMENT CALCULATOR (FIG. 11)
U_{κ_o}
902
912
962
982
ε
980
BASIS FUNCTION INDICATOR

FIG. 9

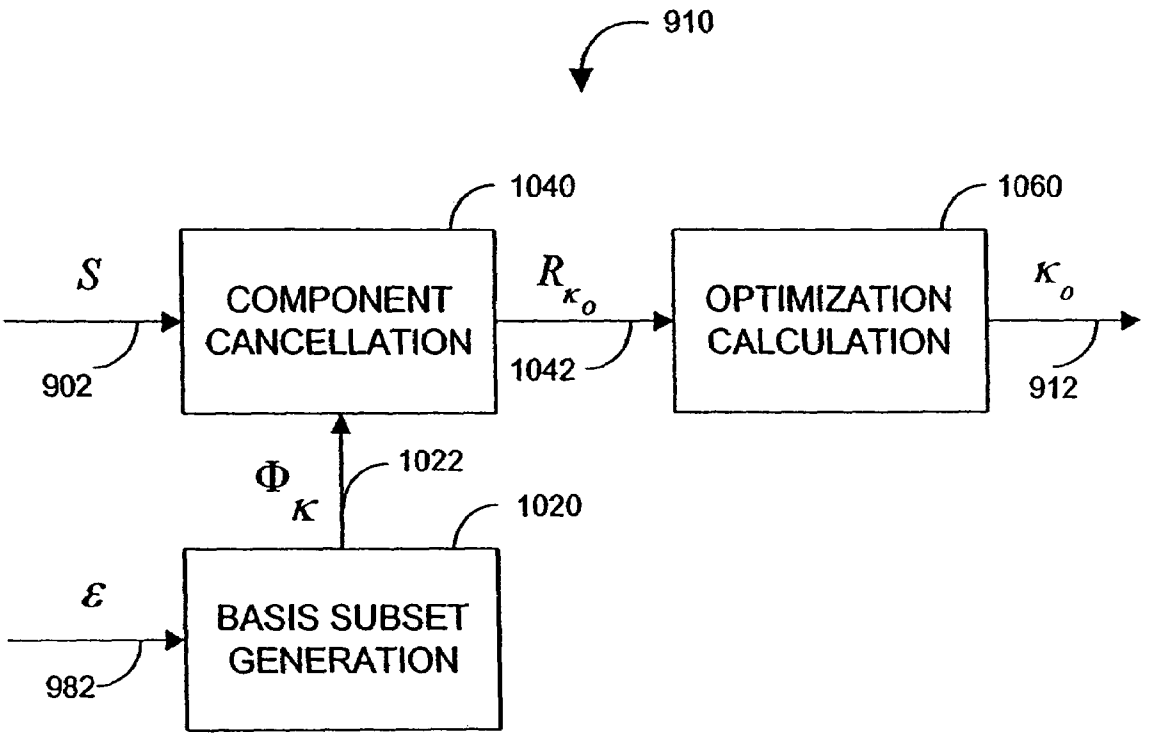
910
1040
1060
S
COMPONENT CANCELLATION
R_{κ_o}
OPTIMIZATION CALCULATION
κ_o
902
1042
912
Φ_κ
1022
1020
ε
BASIS SUBSET GENERATION
982

FIG. 10

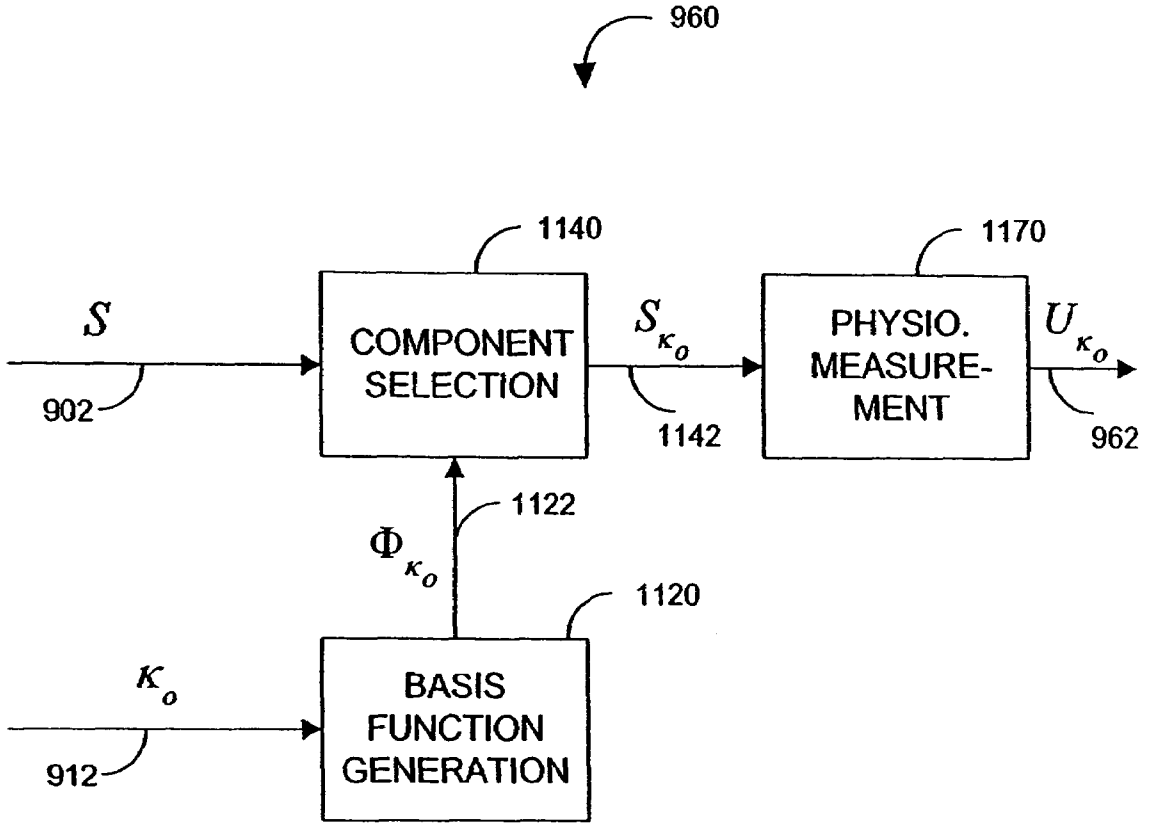
960
1140
1170
S
902
COMPONENT SELECTION
S_{κ_o}
1142
PHYSIO. MEASURE-MENT
U_{κ_o}
962
1122
Φ_{κ_o}
1120
κ_o
912
BASIS FUNCTION GENERATION

FIG. 11

SINE SATURATION TRANSFORM

PRIORITY CLAIM

The present application claims priority benefit under 35 U.S.C. § 120 to, and is a continuation of U.S. patent application Ser. No. 11/417,914, filed May 3, 2006, entitled Sine Saturation Transform," which is a continuation of, U.S. patent application Ser. No. 11/048,232, filed Feb. 1, 2005, entitled Signal Component Processor," which is a continuation of U.S. patent application Ser. No. 10/184,032, filed Jun. 26, 2002, entitled "Signal Component Processor," now U.S. Pat. No. 6,850,787, which claims priority benefit under 35 U.S.C. § 119(e) from U.S. Provisional Application No. 60/302,438, filed Jun. 29, 2001, entitled "Signal Component Processor." The present application also incorporates the foregoing disclosures herein by reference.

CROSS-REFERENCE TO RELATED APPLICATIONS

The following applications are currently pending: U.S. patent application Ser. No. 11/417,914, filed May 3, 2006, entitled Sine Saturation Transform," and U.S. patent application Ser. No. 11/048,232, filed Feb. 1, 2005, entitled Signal Component Processor.

BACKGROUND OF THE INVENTION

Early detection of low blood oxygen is critical in the medical field, for example in critical care and surgical applications, because an insufficient supply of oxygen can result in brain damage and death in a matter of minutes. Pulse oximetry is a widely accepted noninvasive procedure for measuring the oxygen saturation level of arterial blood, an indicator of oxygen supply. A pulse oximeter typically provides a numerical readout of the patient's oxygen saturation and pulse rate. A pulse oximetry system consists of a sensor attached to a patient, a monitor, and a cable connecting the sensor and monitor. Conventionally, a pulse oximetry sensor has both red (RD) and infrared (IR) light-emitting diode (LED) emitters and a photodiode detector. The pulse oximeter measurements are based upon the absorption by arterial blood of the two wavelengths emitted by the sensor. The pulse oximeter alternately activates the RD and IR sensor emitters and reads the resulting RD and IR sensor signals, i.e. the current generated by the photodiode in proportion to the detected RD and IR light intensity, in order to derive an arterial oxygen saturation value, as is well-known in the art. A pulse oximeter contains circuitry for controlling the sensor, processing the sensor signals and displaying the patient's oxygen saturation and pulse rate.

SUMMARY OF THE INVENTION

FIG. **1**A illustrates a plethysmograph waveform **110**, which is a display of blood volume, shown along the ordinate **101**, over time, shown along the abscissa **102**. The shape of the plethysmograph waveform **110** is a function of heart stroke volume, pressure gradient, arterial elasticity and peripheral resistance. Ideally, the waveform **110** displays a short, steep inflow phase **111** during ventricular systole followed by a typically three to four times longer outflow phase **112** during diastole. A dicrotic notch **116** is generally attributed to closure of the aortic valve at the end of ventricular systole.

FIG. **1**B illustrates a corresponding RD or IR sensor signal s(t) **130**, such as described above. The typical plethysmograph waveform **110** (FIG. **1**A), being a function of blood volume, also provides a light absorption profile. A pulse oximeter, however, does not directly detect light absorption and, hence, does not directly measure the plethysmograph waveform **110**. However, IR or RD sensor signals are 180° out-of-phase versions of the waveform **110**. That is, peak detected intensity **134** occurs at minimum absorption **114** and minimum detected intensity **138** occurs at maximum absorption **118**.

FIG. **1**C illustrates the corresponding spectrum of s(t), which is a display of signal spectral magnitude $|S(\omega)|$, shown along the ordinate **105**, versus frequency, shown along the abscissa **106**. The plethysmograph spectrum is depicted under both high signal quality **150** and low signal quality **160** conditions. Low signal quality can result when a pulse oximeter sensor signal is distorted by motion-artifact and noise. Signal processing technologies such as described in U.S. Pat. No. 5,632,272, assigned to the assignee of the present invention and incorporated by reference herein, allow pulse oximetry to function through patient motion and other low signal quality conditions.

Ideally, plethysmograph energy is concentrated at the pulse rate frequency **172** and associated harmonics **174**, **176**. Accordingly, motion-artifact and noise may be reduced and pulse oximetry measurements improved by filtering out sensor signal frequencies that are not related to the pulse rate. Under low signal quality conditions, however, the frequency spectrum is corrupted and the pulse rate fundamental **152** and harmonics **154**, **156** can be obscured or masked, resulting in errors in the computed pulse rate. In addition, a pulse rate, physiologically, is dynamic, potentially varying significantly between different measurement periods. Hence, maximum plethysmograph energy may not correspond to the computed pulse rate except under high signal quality conditions and stable pulse rates. Further, an oxygen saturation value calculated from an optical density ratio, such as a normalized red over infrared ratio, at the pulse rate frequency can be sensitive to computed pulse rate errors. In order to increase the robustness of oxygen saturation measurements, therefore, it is desirable to improve pulse rate based measurements by identifying sensor signal components that correspond to an optimization, such as maximum signal energy.

One aspect of a signal component processor comprises a physiological signal, a basis function index determined from the signal, a basis function waveform generated according to the index, a component derived from the sensor signal and the waveform, and a physiological measurement responsive to the component. In one embodiment, the component is responsive to the inner product of the sensor signal and the waveform. In another embodiment, the index is a frequency and the waveform is a sinusoid at the frequency. In that embodiment, the signal processor may further comprise a pulse rate estimate derived from the signal wherein the frequency is selected from a window including the pulse rate estimate. The physiological measurement may be an oxygen saturation value responsive to a magnitude of the component.

Another aspect of a signal component processor comprises a signal input, a basis function indicator derived from the signal input, a plurality of basis functions generated according to the indicator, a plurality of characteristics of the signal input corresponding to the basis functions and an optimization of the characteristics so as to identify at least one of said basis functions. In one embodiment, the indicator is a pulse rate estimate and the processor further comprises a window configured to include the pulse rate estimate, and a plurality

of frequencies selected from within the window. In another embodiment, the characteristic comprises a plurality of signal remainders corresponding to the basis functions and a plurality of magnitudes of the signal remainders. In that embodiment, the optimization comprises a minima of the magnitudes. In a further embodiment, the characteristic comprises a plurality of components corresponding to the basis functions and a plurality of magnitudes of the components. In this embodiment, the optimization comprises a maxima of the magnitudes.

An aspect of a signal component processing method comprises the steps of receiving a sensor signal, calculating an estimated pulse rate, determining an optimization of the sensor signal proximate the estimated pulse rate, defining a frequency corresponding to the optimization, and outputting a physiological measurement responsive to a component of the sensor signal at the frequency. In one embodiment the determining step comprises the substeps of transforming the sensor signal to a frequency spectrum encompassing the estimated pulse rate and detecting an extrema of the spectrum indicative of the frequency. The transforming step may comprise the substeps of defining a window including the estimated pulse rate, defining a plurality of selected frequencies within the window, canceling the selected frequencies, individually, from the sensor signal to generate a plurality of remainder signals and calculating a plurality of magnitudes of the remainder signals. The detecting step may comprise the substep of locating a minima of the magnitudes.

In another embodiment, the outputting step comprises the substeps of inputting a red (RD) portion and an infrared (IR) portion of the sensor signal, deriving a RD component of the RD portion and an IR component of the IR portion corresponding to the frequency and computing an oxygen saturation based upon a magnitude ratio of the RD component and the IR component. The deriving step may comprise the substeps of generating a sinusoidal waveform at the frequency and selecting the RD component and the IR component utilizing the waveform. The selecting step may comprise the substep of calculating the inner product between the waveform and the RD portion and the inner product between the waveform and the IR portion. The selecting step may comprise the substeps of canceling the waveform from the RD portion and the IR portion, leaving a RD remainder and an IR remainder, and subtracting the RD remainder from the RD portion and the IR remainder from the IR portion.

A further aspect of a signal component processor comprises a first calculator means for deriving an optimization frequency from a pulse rate estimate input and a sensor signal, and a second calculator means for deriving a physiological measurement responsive to a sensor signal component at the frequency. In one embodiment, the first calculator means comprises a signal component transform means for determining a plurality of signal values corresponding to a plurality of selected frequencies within a window including the pulse rate estimate, and a detection means for determining a particular one of the selected frequencies corresponding to an optimization of the sensor signal. The second calculator means may comprise a waveform means for generating a sinusoidal signal at the frequency, a frequency selection means for determining a component of the sensor signal from the sinusoidal signal and a calculator means for deriving a ratio responsive to the component.

BRIEF DESCRIPTION OF THE DRAWINGS

FIGS. **1**A-C are graphical representations of a pulse oximetry sensor signal;

FIG. **1**A is a typical plethysmograph illustrating blood volume versus time;

FIG. **1**B is a pulse oximetry sensor signal illustrating detected light intensity versus time;

FIG. **1**C is a pulse oximetry sensor signal spectrum illustrating both high signal quality and low signal quality conditions;

FIGS. **2**-**3** are magnitude versus frequency graphs for a pulse oximetry sensor signal illustrating an example of signal component processing;

FIG. **2** illustrates a frequency window around an estimated pulse rate; and

FIG. **3** illustrates an associated signal component transform;

FIGS. **4**-**7** are functional block diagrams of one embodiment of a signal component processor;

FIG. **4** is a top-level functional block diagram of a signal component processor;

FIG. **5** is a functional block diagram of a frequency calculator;

FIG. **6** is a functional block diagram of a saturation calculator; and

FIG. **7** is a functional block diagram of one embodiment of a frequency selection;

FIGS. **8**A-B are flowcharts of an iterative embodiment of a frequency calculator; and

FIGS. **9**-**11** are functional block diagrams of another embodiment of a signal component processor;

FIG. **9** is a top-level functional block diagram of a signal component processor;

FIG. **10** is a functional block diagram of an index calculator; and

FIG. **11** is a functional block diagram of a measurement calculator.

DETAILED DESCRIPTION OF THE PREFERRED EMBODIMENTS

FIGS. **2** and **3** provide graphical illustration examples of signal component processing. Advantageously, signal component processing provides a direct method for the calculation of saturation based on pulse rate. For example, it is not necessary to compute a frequency transform, such as an FFT, which derives an entire frequency spectrum. Rather, signal component processing singles out specific signal components, as described in more detail below. Further, signal component processing advantageously provides a method of refinement for the calculation of saturation based on pulse rate.

FIG. **2** illustrates high and low signal quality sensor signal spectrums **150**, **160** as described with respect to FIG. **1**C, above. A frequency window **220** is created, including a pulse rate estimate PR **210**. A pulse rate estimate can be calculated as disclosed in U.S. Pat. No. 6,002,952, entitled "Signal Processing Apparatus and Method," assigned to the assignee of the present invention and incorporated by reference herein. A search is conducted within this window **220** for a component frequency f_o at an optimization. In particular, selected frequencies **230**, which include PR, are defined within the window **220**. The components of a signal s(t) at each of these frequencies **230** are then examined for an optimization indicative of an extrema of energy, power or other signal characteristic. In an alternative embodiment, the components of the signal s(t) are examined for an optimization over a continuous range of frequencies within the window **220**.

FIG. **3** illustrates an expanded portion of the graph described with respect to FIG. **2**, above. Superimposed on the

high signal quality **150** and low signal quality **160** spectrums is a signal component transform **310**. In one embodiment, a signal component transform **310** is indicative of sensor signal energy and is calculated at selected signal frequencies **230** within the window **220**. A signal component transform **310** has an extrema **320** that indicates, in this embodiment, energy optimization at a particular one **330** of the selected frequencies **230**. The extrema **320** can be, for example, a maxima, minima or inflection point. In the embodiment illustrated, each point of the transform **310** is the magnitude of the signal remaining after canceling a sensor signal component at one of the selected frequencies. The extrema **320** is a minima, which indicates that canceling the corresponding frequency **330** removes the most signal energy. In an alternative embodiment, not illustrated, the transform **310** is calculated as the magnitude of signal components at each of the selected frequencies **230**. In that embodiment, the extrema is a maxima, which indicates the largest energy signal at the corresponding frequency. The result of a signal component transform **310** is identification of a frequency f_o **330** determined from the frequency of a signal component transform extrema **320**. Frequency f_o **330** is then used to calculate an oxygen saturation. A signal component transform and corresponding oxygen saturation calculations are described in additional detail with respect to FIGS. **4-8**, below. Although signal component processing is described above with respect to identifying a particular frequency within a window including a pulse rate estimate PR, a similar procedure could be performed on 2PR, 3PR etc. resulting in the identification of multiple frequencies f_{o1}, f_{o2}, etc., which could be used for the calculation of oxygen saturation as well.

Advantageously, a signal component transform **310** is calculated over any set of selected frequencies, unrestricted by the number or spacing of these frequencies. In this manner, a signal component transform **310** differs from a FFT or other standard frequency transforms. For example, a FFT is limited to N evenly-distributed frequencies spaced at a resolution of f_s/N, where N is the number of signal samples and f_s is the sampling frequency. That is, for a FFT, a relatively high sampling rate or a relatively large record length or both are needed to achieve a relatively high resolution in frequency. Signal component processing, as described herein, is not so limited. Further, a signal component transform **310** is advantageously calculated only over a range of frequencies of interest. A FFT or similar frequency transformation may be computationally more burdensome than signal component processing, in part because such a transform is computed over all frequencies within a range determined by the sampling frequency, f_s.

FIGS. **4-7** illustrate one embodiment of a signal component processor. FIG. **4** is a top-level functional block diagram of a signal component processor **400**. The signal component processor **400** has a frequency calculator **410** and a saturation calculator **460**. The frequency calculator **410** has an IR signal input **402**, a pulse rate estimate signal PR input **408** and a component frequency f_0 output **412**. The frequency calculator **410** performs a signal component transform based upon the PR input **408** and determines the f_o output **412**, as described with respect to FIGS. **2-3**, above. The frequency calculator **410** is described in further detail with respect to FIG. **5**, below.

In an alternative embodiment, the frequency calculator **410** determines f_o **412** based upon a RD signal input substituted for, or in addition to, the IR signal input **402**. Similarly, one of ordinary skill in the art will recognize that f_o can be determined by the frequency calculator **410** based upon one or more inputs responsive to a variety of sensor wavelengths.

The saturation calculator **460** has an IR signal input **402**, a RD signal input **404**, a component frequency f_o input **412** and an oxygen saturation output, SAT_{fo} **462**. The saturation calculator **460** determines values of the IR signal input **402** and the RD signal input **404** at the component frequency f_o **412** and computes a ratio of those values to determine SAT_{fo} **462**, as described with respect to FIG. **6**, below. The IR signal input **402** and RD signal input **404** can be expressed as:

$$IR = \begin{bmatrix} IR_0 \\ \vdots \\ IR_{N-1} \end{bmatrix}; \quad RD = \begin{bmatrix} RD_0 \\ \vdots \\ RD_{N-1} \end{bmatrix} \tag{1}$$

where N is the number of samples of each signal input.

FIG. **5** shows one embodiment of the frequency calculator **410**. In this particular embodiment, the frequency calculator functions are window generation **520**, frequency cancellation **540**, magnitude calculation **560** and minima determination **580**. Window generation **520**, frequency cancellation **540** and magnitude calculation **560** combine to create a signal component transform **310** (FIG. **3**), as described with respect to FIG. **3**, above. Minima determination **580** locates the signal component transform extrema **320** (FIG. **3**), which identifies f_o **412**, also described with respect to FIG. **3**, above.

As shown in FIG. **5**, window generation **520** has a PR input **408** and defines a window **220** (FIG. **3**) about PR **210** (FIG. **3**) including a set of selected frequencies **230** (FIG. **3**)

$$\{f_m; m = 0, \ldots M-1\}; \quad f = \begin{bmatrix} f_0 \\ \vdots \\ f_{M-1} \end{bmatrix} \tag{2}$$

where M is the number of selected frequencies **230** (FIG. **3**) within the window **220** (FIG. **3**). Window generation **520** has a sinusoidal output X_f, Y_f **522**, which is a set of sinusoidal waveforms $x_{n,f}$, $y_{n,f}$ each corresponding to one of the set of selected frequencies **230** (FIG. **3**). Specifically

$$X_f = \begin{bmatrix} x_{0,f} \\ \vdots \\ x_{N-1,f} \end{bmatrix}; \quad Y_f = \begin{bmatrix} y_{0,f} \\ \vdots \\ y_{N-1,f} \end{bmatrix} \tag{3a}$$

$$x_{n,f} = \sin(2\pi fn); \quad y_{n,f} = \cos(2\pi fn) \tag{3b}$$

Also shown in FIG. **5**, the frequency cancellation **540** has IR **402** and X_f, Y_f **522** inputs and a remainder output R_f **542**, which is a set of remainder signals $r_{n,f}$ each corresponding to one of the sinusoidal waveforms $x_{n,f}$, $y_{n,f}$. For each selected frequency f **230** (FIG. **3**), frequency cancellation **540** cancels that frequency component from the input signal IR **402** to generate a remainder signal $r_{n,f}$. In particular, frequency cancellation **540** generates a remainder R_f **542**

$$R_f = \begin{bmatrix} r_{0,f} \\ \vdots \\ r_{N-1,f} \end{bmatrix} \tag{4a}$$

-continued

$$R_f = IR - \frac{IR \cdot X_f}{|X_f|^2} X_f - \frac{IR \cdot Y_f}{|Y_f|^2} Y_f \quad (4b)$$

Additionally, as shown in FIG. **5**, the magnitude calculation **560** has a remainder input R_f **542** and generates a magnitude output W_f **562**, where

$$W_f = |R_f| = \sqrt{\sum_{n=0}^{N-1} r_{n,f}^2} \quad (5)$$

Further shown in FIG. **5**, the minima determination **580** has the magnitude values W_f **562** as inputs and generates a component frequency f_o output. Frequency f_o is the particular frequency associated with the minimum magnitude value

$$W_{fo}=\min\{W_f\} \quad (6)$$

FIG. **6** shows that the saturation calculator **460** functions are sinusoid generation **610**, frequency selection **620**, **640** and ratio calculation **670**. Sinusoid generation has a component frequency f_o input **208** and a sinusoidal waveform X_{fo}, Y_{fo} output **612**, which has a frequency of f_o. Frequency selection **620**, **640** has a sensor signal input, which is either an IR signal **202** or a RD signal **204** and a sinusoid waveform X_{fo}, Y_{fo} input **612**. Frequency selection **620**, **640** provides magnitude outputs $z_{IR,fo}$ **622** and $z_{RD,fo}$ **642** which are the frequency components of the IR **202** and RD **204** sensor signals at the f_o frequency. Specifically, from equation 3(a)

$$X_{fo} = \begin{bmatrix} x_{0,fo} \\ \vdots \\ x_{N-1,fo} \end{bmatrix}; \quad Y_{fo} = \begin{bmatrix} y_{0,fo} \\ \vdots \\ y_{N-1,fo} \end{bmatrix} \quad (7)$$

Then, referring to equation 1

$$z_{IR,fo} = \left| \frac{IR \cdot X_{fo}}{|X_{fo}|^2} X_{fo} + \frac{IR \cdot Y_{fo}}{|Y_{fo}|^2} Y_{fo} \right| = \sqrt{\frac{(IR \cdot X_{fo})^2}{|X_{fo}|^2} + \frac{(IR \cdot Y_{fo})^2}{|Y_{fo}|^2}} \quad (8a)$$

$$z_{RD,fo} = \left| \frac{RD \cdot X_{fo}}{|X_{fo}|^2} X_{fo} + \frac{RD \cdot Y_{fo}}{|Y_{fo}|^2} Y_{fo} \right| = \sqrt{\frac{(RD \cdot X_{fo})^2}{|X_{fo}|^2} + \frac{(RD \cdot Y_{fo})^2}{|Y_{fo}|^2}} \quad (8b)$$

For simplicity of illustration, EQS. 8a-b assume that the cross-product of X_{fo} and Y_{fo} is zero, although generally this is not the case. The ratio calculation and mapping **670** has $z_{IR,fo}$ **622** and $z_{RD,fo}$ **642** as inputs and provides SAT_{fo} **262** as an output. That is

$$SAT_{fo}=g\{z_{RD,fo}/z_{IR,fo}\} \quad (9)$$

where g is a mapping of the red-over-IR ratio to oxygen saturation, which may be an empirically derived lookup table, for example.

FIG. **7** illustrates an alternative embodiment of frequency selection **620** (FIG. **6**), as described above. In this embodiment, frequency cancellation **540** and magnitude calculation **560**, as described with respect to FIG. **5**, can also be used, advantageously, to perform frequency selection. Specifically, frequency cancellation **540** has IR **202** and X_{fo}, Y_{fo} **612** as inputs and generates a remainder signal R_{fo} **712** as an output, where

$$R_{fo} = IR - \frac{IR \cdot X_{fo}}{|X_{fo}|^2} X_{fo} - \frac{IR \cdot Y_{fo}}{|Y_{fo}|^2} Y_{fo} \quad (10)$$

The remainder R_{fo} **712** is subtracted **720** from IR **202** to yield

$$Z_{fo} = IR - \left[IR - \frac{IR \cdot X_{fo}}{|X_{fo}|^2} X_{fo} - \frac{IR \cdot Y_{fo}}{|Y_{fo}|^2} Y_{fo} \right] = \frac{IR \cdot X_{fo}}{|X_{fo}|^2} X_{fo} + \frac{IR \cdot Y_{fo}}{|Y_{fo}|^2} Y_{fo} \quad (11)$$

where Z_{fo} **722** is the component of IR **202** at the f_o frequency. The magnitude calculation **560** has Z_{fo} **722** as an input and calculates

$$|Z_{fo}| = \left| \frac{IR \cdot X_{fo}}{|X_{fo}|^2} X_{fo} + \frac{IR \cdot Y_{fo}}{|Y_{fo}|^2} Y_{fo} \right| = \sqrt{\frac{(IR \cdot X_{fo})^2}{|X_{fo}|^2} + \frac{(IR \cdot Y_{fo})^2}{|Y_{fo}|^2}} \quad (12)$$

which is equivalent to equation 8a, above.

FIGS. **8**A-B illustrate an iterative embodiment of the frequency calculator **410** (FIG. **4**) described above. An iterative frequency calculator **410** has an initialization **810**, a signal component transform **820**, an extrema detection **850**, a resolution decision **860** and a resolution refinement **880** and provides a component frequency f_o **870**. Initialization **810** defines a window around the pulse rate estimate PR and a frequency resolution within that window.

As shown in FIG. **8**A, a signal component transform **820** has an initial frequency selection **822**, a frequency cancellation **824** and an magnitude calculation **828**. A decision block **830** determines if the magnitude calculation **828** has been performed at each frequency within the window. If not, the loop of frequency cancellation **824** and magnitude calculation **828** is repeated for another selected frequency in the window. The frequency cancellation **824** removes a frequency component from the IR sensor signal, as described with respect to FIG. **5**, above. The magnitude calculation **828** determines the magnitude of the remainder signal, also described with respect to FIG. **5**, above. If the decision block **830** determines that the remainder signal magnitudes have been calculated at each of the selected frequencies, then the signal component transform loop **820** is exited to the steps described with respect to FIG. **8**B.

As shown in FIG. **8**B, the extrema detector **850** finds a minima of a signal component transform **820** and a resolution decision block **860** determines if the final frequency resolution of a signal component transform is achieved. If not, resolution refinement **880** is performed. If the final resolution is achieved, the component frequency output f_o is equated to the frequency of the minima **870**, i.e. a signal component transform minima determined by the extrema detector **850**.

Further shown in FIG. **8**B, the resolution refinement **880** has a set frequency estimate **882**, a window decrease **884** and a frequency resolution increase **888**. Specifically, the fre-

quency estimate **882** is set to a signal component transform minima, as determined by the extrema detector **850**. The window decrease **884** defines a new and narrower window around the frequency estimate, and the frequency resolution increase **888** reduces the spacing of the selected frequencies within that window prior to the next iteration of a signal component transform **820**. In this manner, a signal component transform **820** and the resulting frequency estimate are refined to a higher resolution with each iteration of signal component transform **820**, extrema detection **850**, and resolution refinement **880**.

In a particular embodiment, the component calculation requires three iterations. A frequency resolution of 4 beats per minute or 4 BPM is used initially and a window of five or seven selected frequencies, including that of the initial pulse rate estimate PR, is defined. That is, a window of either 16 BPM or 24 BPM centered on PR is defined, and a signal component transform is computed for a set of 5 or 7 selected frequencies evenly spaced at 4 BPM. The result is a frequency estimate f_1. Next, the frequency resolution is reduced from 4 BPM to 2 BPM and a 4 BPM window centered on f_1 is defined with three selected frequencies, i.e. f_1-2 BPM, f_1, and f_1+2 BPM. The result is a higher resolution frequency estimate f_2. On the final iteration, the frequency resolution is reduced to 1BPM and a 2 BPM window centered on f_2 is defined with three selected frequencies, i.e. f_2-1 BPM, f_2, and f_2+1 BPM. The final result is the component frequency f_o determined by a signal component transform to within a 1BPM resolution. This component frequency f_o is then used to calculate the oxygen saturation, SAT_{fo}, as described above.

The signal component processor has been described above with respect to pulse oximetry and oxygen saturation measurements based upon a frequency component that optimizes signal energy. The signal component processor, however, is applicable to other physiological measurements, such as blood glucose, carboxy-hemoglobin, respiration rate and blood pressure to name a few. Further, the signal component processor is generally applicable to identifying, selecting and processing any basis function signal components, of which single frequency components are one embodiment, as described in further detail with respect to FIG. **9**, below.

FIGS. **9-11** illustrate another embodiment of a signal component processor **900**. As shown in FIG. **9**, the processor **900** has an index calculator **910** and a measurement calculator **960**. The index calculator has a sensor signal input S **902** and outputs a basis function index κ_o **912**, as described with respect to FIG. **10**, below. The measurement calculator **960** inputs the basis function index κ_o **912** and outputs a physiological measurement U_{κ_o} **962**, as described with respect to FIG. **11**, below. The processor **900** also has a basis function indicator **980**, which is responsive to the sensor signal input S **902** and provides a parameter ϵ **982** that indicates a set of basis functions to be utilized by the index calculator **910**, as described with respect to FIG. **10**, below.

As shown in FIG. **10**, the functions of the index calculator **910** are basis subset generation **1020**, component cancellation **1040** and optimization calculation **1060**. The basis subset generation **1020** outputs a subset Φ_κ **1022** of basis function waveforms corresponding to a set of selected basis function indices κ. The basis functions can be any complete set of functions such that

$$S = \sum_\kappa a_\kappa \Phi_\kappa \tag{13}$$

For simplicity of illustration purposes, these basis functions are assumed to be orthogonal

$$\langle \vec{\Phi}_\gamma, \vec{\Phi}_\eta \rangle = 0; \gamma \neq \eta \tag{14}$$

where < > denotes an inner product. As such

$$a_\kappa = \langle S, \Phi_\kappa \rangle / \langle \Phi_\kappa, \Phi_\kappa \rangle \tag{15}$$

$$S_\kappa = a_\kappa \Phi_\kappa \tag{16}$$

In general, the basis functions may be non-orthogonal. The subset of basis functions generated is determined by an input parameter ϵ **982**. In the embodiment described with respect to FIG. **5**, above, the basis functions are sinusoids, the indices are the sinusoid frequencies and the input parameter ϵ **982** is a pulse rate estimate that determines a frequency window.

As shown in FIG. **10**, the component cancellation **1040** generates a remainder output R_κ **1042**, which is a set of remainder signals corresponding to the subset of basis function waveforms Φ_κ **1022**. For each basis function waveform generated, component cancellation removes the corresponding basis function component from the sensor signal S **902** to generate a remainder signal. In an alternative embodiment, component cancellation **1040** is replaced with a component selection that generates a corresponding basis function component of the sensor signal S **902** for each basis function generated. The optimization calculation **1060** generates a particular index κ_o **912** associated with an optimization of the remainders R_κ **1042** or, alternatively, an optimization of the selected basis function signal components.

As shown in FIG. **11**, the functions of the measurement calculator **960** are basis function generation **1120**, component selection **1140**, and physiological measurement calculation **1170**. The component selection **1140** inputs the sensor signal S **902** and a particular basis function waveform Φ_{κ_o} **1122** and outputs a sensor signal component S_{κ_o} **1142**. The physiological measurement **1170** inputs the sensor signal component S_{κ_o} **1142** and outputs the physiological measurement U_{κ_o} **962**, which is responsive to the sensor signal component S_{κ_o} **1142**. In the embodiment described with respect to FIG. **6**, above, the basis functions Φ_κ are sinusoids and the index κ_o is a particular sinusoid frequency. The basis function generation **1120** creates sine and cosine waveforms at this frequency. The component selection **1140** selects corresponding frequency components of the sensor signal portions, RD and IR. Also, the physiological measurement **1170** computes an oxygen saturation based upon a magnitude ratio of these RD and IR frequency components.

The signal component processor has been disclosed in detail in connection with various embodiments. These embodiments are disclosed by way of examples only and are not to limit the scope of the claims that follow. One of ordinary skill in the art will appreciate many variations and modifications.

What is claimed is:

1. A method for filtering a physiological signal to improve a calculation of a pulse rate, the method comprising:

obtaining within a patient monitor a signal indicative of pulse rate information of a patient being monitored;

obtaining an initial frequency estimate of a pulse rate of the patient with a processor;

combining at least one sinusoidal waveform with said signal to produce a predetermined response; and

signal component processing the combined signal with the processor to determine said pulse rate.

2. The method of claim **1**, comprising generating one or more sinusoidal waves as the at least one sinusoidal waveform.

3. The method of claim **2**, comprising individually canceling the generated sinusoidal waves from the signal.

4. The method of claim **1**, wherein said signal component processing includes determining a frequency corresponding to the sinusoidal waveform which produces an extrema.

5. The method of claim **1**, comprising segmenting the signal into at least one pulse rate cycle.

6. The method of claim **4**, wherein the extrema comprises a minima.

7. The method of claim **1**, wherein said signal component processing includes determining an oxygen saturation.

8. A signal component processor capable of determining a pulse rate of a patient being monitored, the processor comprising:

at least one input capable of receiving a signal indicative of pulse rate information of a patient being monitored; and

a frequency calculator configured to determine an initial frequency estimate of a pulse rate of the patient, configured to combine at least one sinusoidal waveform with said signal to produce a predetermined response, and configured to component process the combined signal to determine said pulse rate.

9. The processor of claim **8**, wherein the frequency calculator is further configured to generate one or more sinusoidal waves as the at least one sinusoidal waveform.

10. The processor of claim **9**, wherein the frequency calculator is further configured to individually cancel the generated sinusoidal waves from the signal.

11. The processor of claim **8**, wherein the frequency calculator is further configured to determine a frequency corresponding to the sinusoidal waveform which produces an extrema.

12. The processor of claim **11**, wherein the extrema comprises a minima.

13. The processor of claim **8**, wherein the frequency calculator is further configured to segment the signal into at least one pulse rate cycle.

14. The processor of claim **8**, comprising a saturation calculator configured to process said at least one input signal using said pulse rate to determine an oxygen saturation of the patient.

* * * * *